Nanocomposite Protective Coatings Based on Ti–N–Cr/Ni–Cr–B–Si–Mo, their Structure and Properties[1]

A.D. Pogrebnjak*,**, M.M. Danilionok***, A.A. Drobyshevskaya*,**, V.M. Beresnev*,***, N.K. Erdybaeva****, G.V. Kirik**, S.N. Dub*****, V.S. Rusakov******, V.V. Uglov***, A.P. Shypylenko*,***, P.V. Zukovski*******, and Yu.N. Tuleushev*******

*G.V. Kurdyumov Institute for Metal Physics, NAS Ukraine, Sumy, Ukraine
**Sumy Institute for Surface Modification, PO BOX 163, Sumy, Ukraine
***Belarus State University, Minsk, Belarus
****East-Kazakstan State Technical University, Ust'-Kamenogorsk, Kazakstan
*****Institute Super Hard Materials NAS Ukraine, Kiev, Ukraine
******Moscow State University, Moscow, Russia
*******Institute for Nuclear Physics, Almaty, Kazakstan
********Lublin Technical University, Lublin, Poland

Abstract – First results on manufacturing and investigations of a new type nanocomposite, protective coatings are presented. They were manufactured using a combination of two technologies: plasma-detonation coating deposition with the help of plasma jets and thin coating vacuum-arc deposition. We investigated structure, morphology, physical and mechanical properties of the coatings of 80 to 90 μm thickness, as well as defined the hardness, elastic Young modulus and their corrosion resistance in different media. Grain dimensions of the nanocomposite coatings on Ti–N–Cr base varied from 2.8 to 4 nm. The following phases and compounds formed as a result of plasma interaction with the thick coating surface were found in the coatings: Ti–N–Cr (220), γ-Ni_3–Fe, a hexagonal Cr_2–Ti, Fe_3–Ni, (Fe, Ni)N and the following Ti–Ni compounds: Ti_2Ni, Ni_3Ti, Ni_4Ti, etc. We also found that the nanocomposite coating microhardness increased to (32 ± 1.1) GPa. The Young elastic modulus was determined to be (320 ± 20) GPa – it was derived from the loading-unloading curves. The protective coating demonstrated the increased corrosion resistance in acidic and alkaline media in comparison with that of the stainless steel substrate.

1. Introduction

It is well known that investigations of nanostructured objects are the most quickly progressing field in a modern material science, since a superfine disperse structure can provide a significant and, in some cases, crucial changing of material properties [1, 2].

Investigations of materials with a superfine grain structure demonstrated that a decrease in crystal grain dimensions below some "threshold value" crucially changed the material properties. These "dimension effects" demonstrated themselves even in the case, when an average crystal grain dimension did not exceed 100 nm, but became more pronounced when their dimensions were 10 nm, and the intercrystalline (intergrain) distances ranging within the units of a nanometer contained mainly amorphous phases (nitrides, oxides, carbides, etc.). A strength existing inside these interfaces contributes to an increase in the nanocomposite coating deformation resistance, but an absence of dislocations inside the crystallites provides an increase in the coating elasticity [3–5].

In this work, we present investigation results for the structure and properties of new type nanocomposite protective coatings on Ti–N–Cr/Ni–Cr–B–Si–Fe base, which were treated with the help of a plasma-detonation technology and coated with a thin Ti–Cr–N of 2.4 to 3 μm thickness using a vacuum-arc deposition. A purpose of this work was manufacturing and investigation of the structure, physical and mechanical properties of the nanocomposite protective coatings Ti–N–Cr/Ni–Cr–B–Si–Fe of 80 to 120 μm thickness.

2. Methods of sample manufacturing and analysis

Rods of a stainless steel 12X18T (321 stainless steel), were rolled and then we cut samples of 2×20×20 mm dimensions. Further, the samples were annealed, to remove the cold working effects and defects. Thereafter, the samples were coated by a powder PG-19N-01 till 29–68 μm thickness. The powder composition was: Ni – the base, Cr – 8 to 14%, Si – 2.5 to 3.2%, B – about 2%, Fe – about 5%. Using the Plasmatron "Impulse-6" [6–8], we further deposited the coating till 120 μm thickness (under the following conditions: the powder fraction was 63 to 80 μm, the powder expenditures – about 22.5 g/min, the pulse repetition frequency – 4 Hz). The plasma jet re-melted the surface layer was performed without the powder, but with an eroding W

[1] This work was funded by two projects: ISTCs K-1198 and NAS of Ukraine "Nano-Systems, Nano-Materials, and Nano-Technologies".

electrode. All the samples were coated by Ti–N–Cr of 2.4 μm thickness using the vacuum-arc source, in vacuum, during 1 min (10–3 Pa), under titanium cathode arc burning current 100 A and basic voltage 1 kV. The coating deposition was performed inside a device chamber under 10^{-1} Pa pressure, the arc burning current of chromium and titanium cathodes being 100 A and the basic voltage – 120 V. The time for the fine coating deposition was 10 min.

To investigate the element composition we applied the Rutherford ion back scattering of 2.35 MeV $^4He^+$ ion energies and 2.012 MeV proton energies (Dubna, JINR) [9]. The morphology and element composition analyses were performed using a scanning electron microscope REMMA-103M with a microanalyzer (EDS-energy dispersion and WDS-wave dispersion spectra). The structure and phase composition were studied using the device Advance 8 (XRD-analysis) including also a sliding beam [21]. A microanalysis was performed using a spectral electron microscope LEO-1455R, which passed across the cross-section width (across the fine and the thick coating, which were treated under various experimental conditions without melting and with plasma jet melting) [21].

We performed electro-chemical corrosion tests in 1% NaCl medium using PCI 4/300 potentiometer-galvanometer ZRA and corrosion cells. Further, applying electrochemical program software DS-105, we obtained experimental dependences and Tafel curves.

In the other part of tests we used a NaCl 2% solution under T = 18 °C – we determined corrosion rates, corrosion potentials and currents, and Tafel coefficients All the potentials were presented with a reference to a calomel electrode. Additionally, we obtained the cyclic volt-ampere characteristics for the samples exposed to 1 M H_2SO_4 and 1 M NaOH solutions. Hardness tests were performed with a three-face Berkovich indentation using a nanometer Nanoindentor II (MTS Systems Corporation, Oak Ridge, TN USA) [6, 10].

In the process of testing with high accuracy, we registered a dependence of the Berkovich indentor top motion on a load. An accuracy of a measured indentation depth was equal to ± 0.04 nm of an indentation load (± 75 nN). The device was able to do about 3 load measurements, and the indentor displacement for 1 s, and, to reduce vibrations, it was mounted to a vibration-isolating table. In every test, the indentor was loaded and unloaded three times, every time the load was higher, but did not exceed 5 μN (= 0.5 G), the depth remaining 150 N.

Mössbauer spectra (MS-spectra) were taken by detecting the γ-quanta in transition geometry. The MS-spectra were taken for the powders prepared from chips, which were cut from the fine coating surfaces and partially from the thick coating stainless steel samples. All the spectra were treated using restoration of distribution functions of two fine parameters (efficient magnetic field H, quadrupole shift ε, and a Mössbauer line δ [11]). Relative efficiency of the partial Mössbauer spectra was determined in assumption that dynamical characteristics of Fe atoms in various positions remained unchanged, according to the relative phase content (in units of atomic iron) or to Fe atom quantities in various positions.

3. Results and discussion

Figure 1, *a* presents an image of the nanostructured composite protecting TiNCr coating surface region.

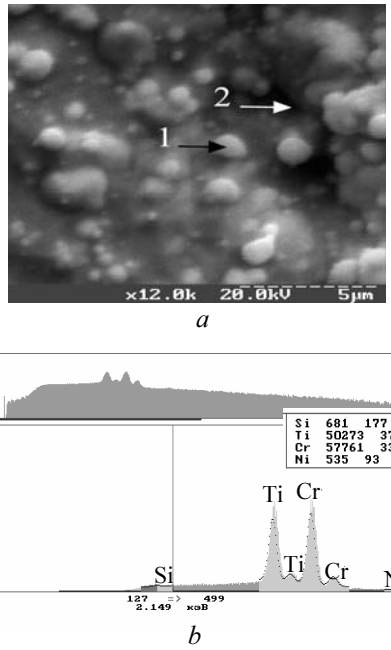

a

b

Fig. 1

In this coating surface one can see some regions of a droplet fraction (they are marked with points, at which we performed microanalysis). The point 1, which was taken in the coating surface in X-ray energy dispersion spectrum shows Si, Ti, Cr, and Ni traces. Figure 1, *b* and Table 1 show results of integral and local analyses. The results demonstrated almost the same picture for Si (from 0.56 to 0.58%), Ti (from 39 to 41%), Cr (56.8 to 59.4%) and Ni thick coating (0.82 to 0.98%) concentration.

Table 1

Points	Ni	Si	Ti	Cr	Σ
p19_int1	0.578	40.509	58.095	0.819	100.000
p19_int2	0.487	41.867	56.797	0.850	100.000
p19_2	0.564	39.073	59.390	0.973	100.000
p19_1	0.507	40.711	57.805	0.978	100.000

Figures 2 show Rutherford back-scattering spectra (RBS) for protons (Fig. 2, *a*) and helium ions $^4He^+$ (Fig. 2, *b*). From these spectra one can see that all the elements composing this coating TiNCr/Ni–Cr(Si, B, Fe); N, O, Ti, Cr were found in it. The fact that

a "step" was present in the spectrum almost over the whole depth of analysis in this coating is worth one's attention. It indicates a uniform nitrogen distribution and formation of Ti_2, Cr_xN_{1-x} compounds.

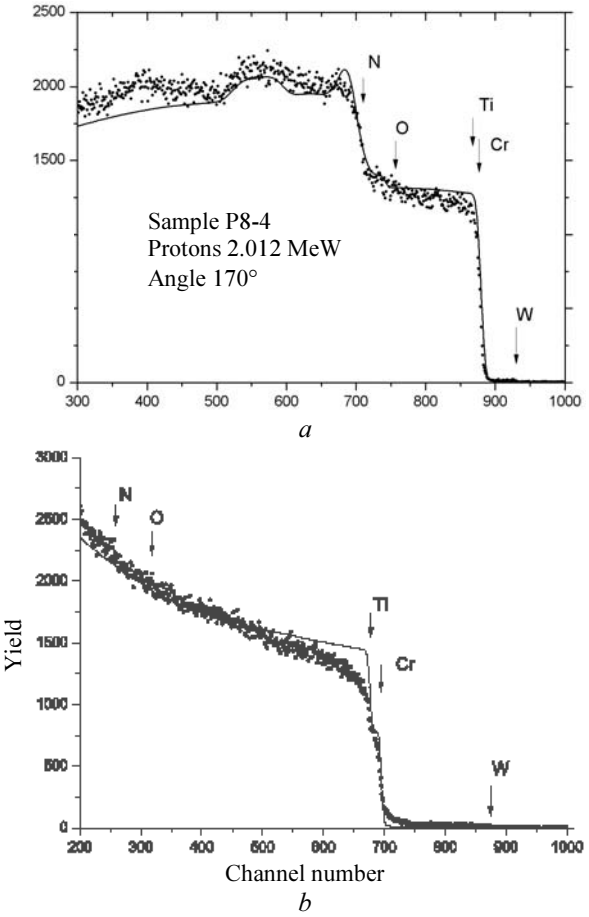

Fig. 2

A stoichiometry of the assumed compound was close to $Ti_{40}Cr_{40}N_{20}$ or $(Ti, Cr)_2N$ [13, 19]. Figure 3, *b* shows that the peaks for titanium and chromium were shifted a little and formed a step near the thin coating surface, which also indicated the formation of Ti_xCr_{1-x} compound in the layer of about several tens of a micrometer.

Table 2 demonstrates the coating composition obtained using the RBS data and a standard program [9].

Table 2

Depth concentration, at %						
at:A^2	W	Ni	Cr	Ti	O	N
500.0	.07	.00	38.70	38.70	11.26	11.26
1000.0	.07	.00	38.70	38.70	9.01	13.51
1850.0	.09	.00	38.70	38.70	4.50	18.02
2850.0	.09	.00	38.70	38.70	2.25	20.27
11850.0	.00	61.30	38.70	.00	.00	.00

Figures 3 present a general view of these coatings (their cross sections).

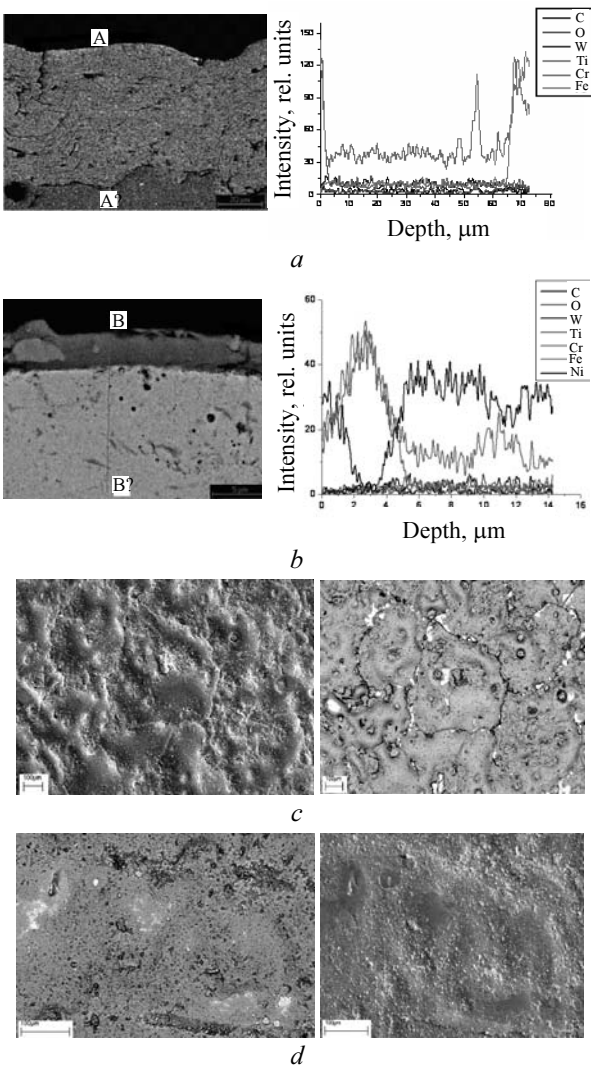

Fig. 3

One can also mention a low W concentration (0.07 at %) found in the thin coating. But near the interface between the thick and thin coatings this concentration increased to 0.1 at %. We assumed that W came from the thick coating (from the eroding electrode). The stainless steel substrate composition demonstrated the ratio $Ni_{61}Cr_{39}$ (i.e., the compound being close to $Ni_{61}Cr_{39}$ composition was formed in the substrate).

Figure 3, *a* shows the sample without coating. The right part of this Figure demonstrates the results of micro-analysis (A–A′ cross section). An etched coatings layer is almost without pores. The interface between the coating and the substrate is wavy, which indicates a penetration of the powder particles to the substrate.

Figure 3, *b* shows a cross section for Ti–N–Cr/Ni–Cu–B–Si–Fe coating. Its element distribution over the cross-section depth is demonstrated in the right part (B–B′). The thin coating was composed of Ti, Cr (N was not found, possibly due to low detector resolution). If to compare the surface images in Figures 3, *c*

and *d*, both under some trivial conditions and using an element contrast, one would pay attention to the difference in the element distribution observed in the surface. In the case of a melted thick coating surface, one observed an element distribution occurring in the boundaries of the melting zones and the element mass-transfer came from the thick coating bulk. The results of XRD analysis for TiCrN/Ni–Cr coating are presented in the

Table 3 treatment of the diffraction patterns demonstrated (Ti, Cr)N (200), (Ti, Cr)N (220) and γ-Fe_3Ni_3 phases, in the samples N8 and N10 we found additionally (Ti, Cr)Ni with $FeNi_3$ phase. Also we found a shift of the diffraction peaks, the variations of under-peak area and of the intensities ratios. Measurements and analysis of the diffraction lines taken with a sliding beam demonstrated the peak smearing, which indicated amorphization or formation of nanocrystal phases.

Table 3

Degree 2θ	Area	Intensity	Half-width
42.830	53.210	65	1.5756
44.270	27.609	108	0.4965
51.520	7.540	38	0.3850
76.000	12.300	28	0.8400
92.420	6.083	28	0.4200
97.740	2.357	24	0.2000
Value Angstrom	Relative intensity	Phase	HKL
2.1113	60.19	(Ti, Cr)N	200
2.0459	100.00	$FeNi_3$	111
1.7738	35.19	$FeNi_3$	200
1.2521	25.93	$FeNi_3$	220
1.0679	25.93	$FeNi_3$	311
1.0235	22.22	$FeNi_3$	222

Measurements of the X-ray diffraction performed at 0.5° angle demonstrated that in addition to the basic phases there were present also simple hexagonal Cr_2Ti, Fe_3Ni (Fe, Ni) and various compounds of titanium with nickel Ti_2Ni, Ni_3Ti, Ni_4Ti_3, etc. Formation of an additional phase occurred at some initial stages of coating deposition as a result of titanium, nickel, chromium, and iron diffusion. The resulting solid solution is stated to be a small-grain dispersion one (the grain dimensions were calculated according to the formula Debai–Sherer and reached about 2.8 to 4 nm).

A comparison of X-ray spectra obtained for the samples N8 and N10 after melting the PG-19N-01 sample by a plasma jet with a subsequent deposition of a thin TiNCr coating did not demonstrate a difference in the phase compositions.

A partial spectrum I corresponds to a stainless steel. Some asymmetry, which was observed in a quadrupole duplet (various amplitudes and widths, but similar areas of the resonance lines) was due to a non-uniformity in surrounding Fe atoms.

A partial spectrum II corresponds to α-Fe particles. In comparison with a standard α-Fe spectrum these values of the Mössbauer line shift δ and those for the quadrupole one ε, which differed from zero, and a little lower value of the superfine field indicated the presence of nanodimension impurities ≤ 100 nm (in the locally non-uniform systems) are present in Table 4 [11].

Table 4

Cast	I			II			
	δ, mm/s	ε, mm/s	*I*, %	δ, mm/s	ε, mm/s	H_n, kE	*I*, %
Substrate	1 –0.090	1 –0.090	100	–	–	–	–
Coating with substrate	2 –0.084	2 –0.087	2.2 94.4	3 –0.04	2 –0.03	2 327	6 5.6

The morphology of the coating surface and the cross-sections were studied additionally using an electron scanning microscopy and an X-ray spectral micro-analysis (using LEO-1455 R microscope).

The thin coating (Ti, Cr)N on a basis of a solid solution repeats fully the substrate relief.

Samples with (Ti, Cr)N coating had 6.8 and 8.4 mkg/h corrosion rate, depending on the thin layer composition (the stoichiometry). Investigation results for the cyclic volt-ampere characteristics of samples with Ti–Cr–N/Ni–Cr–B–Si–Fe (Mo, W) coatings, which were placed in different media (*a* – for 1M H_2SO_4; *b* – for 3% NaCl; *c* – for 1M NaOH) show that the best corrosion resistance characteristics were found in the coatings with the stoichiometry being close to Ti_{25}–Cr_{25}–N_{50}, depending on a reference voltage.

Figure 5 shows the hardness *H* and the elastic modulus *E* determined using a nanohardness meter (Nanoindenter II) according to Oliver and Pharr methods [9, 11] and with the help of Berkovicz indenter.

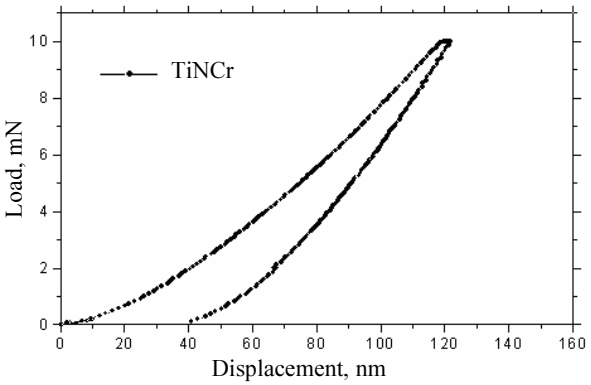

Fig. 5

For the surface layer the value of elastic recovery W_e was calculated using the loading-unloading curves, according to the formula

$$W_e = \frac{h_{\max} - h_r}{h_{\max}}, \quad (1)$$

where h_{max} is the maximum penetration depth; h_r is the residual depth after the load relieve.

It was obtained that the elastic modulus of (Ti, Cr)N coating had the value $E_{mean} \sim 318$ GPa, its hardness being 31.6 GPa, and maximum value – 32.7 GPa (are present in Table 5).

Table 5

Coatimgs	*E*, GPa	*H*, GPa
TiNCr	319 ± 27	31.6 ± 1.1

4. Conclusions

First results on manufacturing of nanocomposite, combined, protective coatings on Ti–N–Cr/Ni–Cr–B–Si–Fe (Mo, W) base are presented.

It was demonstrated that the nanodimension grains (2.8 to 4 nm) and the phases Cr_2Ti, Fe_3Ni, Ti_2Ni, NiTi, Ni_4Ti_3, etc. were formed in the solid solution (Ti, Cr)N. The coating hardness reached (32.6 ± 1.1) GPa, the elastic modulus amounting (320 ± 20) GPa. It was found that the studied coating had a high corrosion resistance in acidic and alkaline media. The resulting coating had also a high layers adhesion (between thin and thick coatings), as well as a high resistance to a cylinder friction over the sample surface.

Acknowledgements

The authors are thankful to Prof. Yu.N. Tyurin, Dr. O.V. Kolisnichenko for their help in sample preparation, to Dr. S.B. Kislitsyn for corrosion tests.

References

[1] A. Gavaleiro and J.T. Hosson, *Nanostructured Coating*, Berlin, Springer-Verlag, 2006.

[2] A.A. Voevodin, D.V. Shtansky, E.A. Levashov, and J.J. Moore, *Nanostructured Thin Films and Nanodispersion Strengthened Coatings*, Dordrecht, Kluger Academic, 2004.

[3] E.A. levashov and D.V. Shtansky, Uspekhi Khimii **76**(5), 501–509 (2007).

[4] E.N. Reshetnyak and V.E. Strelnitsky, *in Sintez Nanostructurirovannykh Plionok: Dostizhenija I Perspektivy. Kharkov Nanotechnology Assembly*, Nanostructurirovannyje Materialy, Kharkov, 2007, Vol. 1, pp. 6–16.

[5] D.V. Shtansky, M.I. Petrazhik, I.A. Bashkova et al., FTT, Phys. Stat. Sol. **48**/7, 1231–1238 (2006) [Russian].

[6] V.M. Beresnev, A.D. Pogrebnjak, N.A. Azarenkov et al., Physical Surface Engineering, Kharkov, 2007, Nos. 1–2, pp. 4–27.

[7] K.K. Kadyrzhanov, F.F. Komarov, A.D. Pogrebnjak et al., *Ion-Beam and Ion-Plasma Treatment of Materials*, Moscow, MSU, 2005, 640 pp.

[8] A.D. Pogrebnjak and Yu.N. Tyurin, Usp. Fiz. Nauk **175**, 517–543 (2005).

[9] L. Feldman and D. Mayer, *Osnovy Analiza Poverkhnosti i Tonkikh Plionok*, Moscow, Mir, 1989, 342 pp.

[10] W. Oliver and G.M. Pharr, J. Mater. Res. **7**/6, 1364–1586 (1992).

[11] N.A. Azarenkov, V.M. Beresnev, and A.D. Pogrebnjak, *Structure and Properties of coatings and modified Layers of Materials*, Kharkov, Kharkov National University, 2007, 565 pp.